CRYSTAL GROWTH & DESIGN

Article

pubs.acs.org/crystal

Unusual Chemical Ratio, Z″ Values, and Polymorphism in Three New *N*-Methyl Aminopyridine−4-Nitrophenol Adducts

Published as part of the Crystal Growth & Design Mikhail Antipin Memorial virtual special issue

Sergiu Draguta,[*,†] Andrey A. Yakovenko,[‡] Marina S. Fonari,[†,§] and Tatiana V. Timofeeva[†]

[†]Department of Chemistry & Biology, New Mexico Highlands University, Las Vegas, New Mexico 87701, United States

[‡]X-ray Science Division Argonne National Laboratory 9700 South Cass Avenue, Building 401 MS-16, Argonne, Illinois 60439, United States

[§]Institute of Applied Physics Academy of Sciences of Moldova, Academy Street 5 MD2028, Chisinau, Moldova

Supporting Information

ABSTRACT: Cocrystallization of 4-nitrophenol (**I**) with *N*-methyl substituted aminopyridines, 4-*N*-methylaminopyridine **1**, 2-*N*-methylaminopyridine **2**, and 2-*N*,*N*-dimethylaminopyridine **3**, resulted in three novel adducts **1**·2(**I**), **2**·3(**I**), and **3**·3(**I**), one of which, **2**·3(**I**), was found in three polymorphic forms, **A**, **B**, and **C**. The single crystals were grown by slow evaporation from ethanol. The proton transfer from the phenoxy to the pyridine moieties was registered in all compounds. The adducts comprise pyridinium cations, 4-nitrophenolate anions, and varying in number neutral 4-nitrophenol molecules. Though the asymmetric hydrogen-bonded network involving the $-N^{+}H$ groups of pyridinium cations and the $-C-O^{-}$ and $-C-OH$ groups of 4-nitrophenol moieties is registered in the adducts, the delicate balance of noncovalent interactions that include CH···O hydrogen bonds and face-to-face stacking interactions between the extended antiparallel arrays of components controls the centrosymmetric packing. Although three polymorphs of **2**·3(**I**) share several structural common features, they reveal significant differences in the conformation of the pyridinium cation, and the hydrogen-bonding patterns.

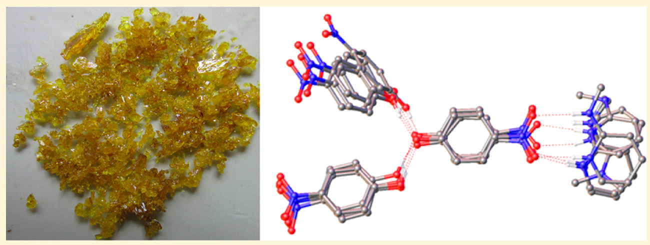

■ INTRODUCTION

Products of supramolecular synthesis such as cocrystals, salts, and solvates find a wide range of applications in different domains. For example, pharmaceutical cocrystals are intensively elaborated nowadays, since the active pharmaceutical ingredients (API) they include do not change their molecular structure but improve some physicochemical properties targeted by the particular problem.[1−3] In area such as nonlinear optics (NLO), salts often represent more prospective materials because ionic components possess larger molecular hyperpolarizability than neutral molecules.[4−6] Since Etter's pioneering work,[7] many attempts to develop strategies to increase the probability of formation of acentric crystals have been made. For these purposes the analysis of the regularities of crystal packing based on the statistics extracted from CSD, in particular, the data on the most frequently encountered space groups, correlations between the inherent molecular and crystal symmetries, and the supramolecular synthons responsible for intermolecular interactions are of considerable importance.[7−10] Along with several other groups, M. Antipin with co-workers have carried out the structural analysis of the polymorphic centric−acentric pairs using the CSD resources and concluded that generation of the stable acentric supramolecular synthons is a reliable prerequisite for the growth of acentric crystal by choosing appropriate crystallization conditions.[11−13]

4-Nitrophenol derivatives are forthcoming components for NLO materials, since they possess a typical linear donor−π-acceptor conjugated chain, and are prone to the formation of strong hydrogen bonds. This combination may result not only in hydrogen bonding, but also in proton transfer, which could further increase molecular hyperpolarizability.[6,14] Adducts of 4-nitrophenol with *N*-bases, including positional isomers of aminopyridines and alkyl-substituted aminopyridines, were proposed as good candidates for NLO application due to their predisposition to form acentric crystals with varying molar ratios.[14−16] In order to explain the acentricity of these salts, Prakash et al. suggested that predominantly *ortho*-aminopyridines with adjacent pyridine and amino-binding sites act as efficient molecular building block for the helical assembly.[14] Having been encouraged by that research we have also synthesized, studied, and reported on the acentric materials composed of 4-nitrophenol and other aminopyridine derivatives.[17] The CSD survey reported by us demonstrated that the tricomponent *N*-base-4-nitrophenolate-4-nitrophenol systems more likely form acentric crystals than the binary *N*-base-4-nitrophenol adducts. We have speculated that this preference

Received: March 15, 2014
Revised: April 30, 2014
Published: May 14, 2014

results from the helicity induced by the H-bonded 4-nitrophenol-4-nitrophenolate supramolecular fragments. The isomorphism, demonstrated by the two groups of compounds, including the new structures, as well as the previously reported ones, supported that hypothesis.

In continuation of those studies, the single crystals of 4-nitrophenol with mono- and dimethyl-substituted *N*-amino-pyridines (Scheme 1) have been grown.

Scheme 1. Co-Formers Used in This Study and the Molar Ratio in the Final Products

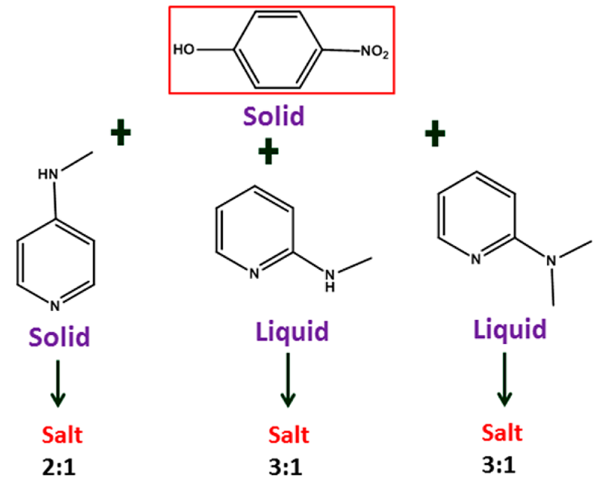

The methyl-*N*-aminopyridines were chosen to investigate how their basic properties enhanced by incorporation of electron donor methyl groups are manifested in the presence of secondary (NHMe) or tertiary (NMe_2) amino groups and how they influence the crystal packing with an emphasis on the possible acentricity. The fact that two of the three starting *N*-bases are liquids at room temperature (Scheme 1) is usually considered as an impediment for the cocrystallization process that requires special crystallization conditions. Supramolecular synthesis, allowing solidification of the liquids, or a non-congruently soluble cocrystal component pair[18] reveals a new range of possible applications for such components. Although examples of inclusion of single liquid compound to solid adduct are documented,[19−23] it is known that cocrystallization becomes particularly difficult when two components differ essentially in solubility, since the least soluble component might precipitate out exclusively.[24] The high difference in solubility of starting compounds usually leads to polymorphism of the final crystal material and unexpected stoichiometry[18,25] with high Z′ values (defined as the number of formula units in the asymmetric unit),[26,27] despite the fact that some recent findings demonstrate the possibilities for controlling multiple stoichio-metries by such methods as grinding and liquid assisted grinding,[28] evaporation of solutions of varying concentrations,[29] evaporation of solutions at different temperatures,[30] or cocrystallization by freeze−drying.[31] The most recent example revealing the successful solidification of the liquid anesthetic drug propofol (2,6-diisopropylphenol) represents its cocrystal-lization with isonicotinamide. The final binary system drug:cocrystal formerly has 3:2 stoichiometry and exists as three temperature-dependent "isostructural" polymorphs re-taining the hydrogen-bonded synthons and key packing features across three forms.[23] According to the current concepts, the origins of polymorphism lie either in molecular conformational flexibility[32−34] or in the distinctions in the hydrogen-bonding systems for rigid molecules.[35]

In the present work, cocrystallization of 4-nitrophenol (**I**) with three *N*-methyl substituted aminopyridines, viz., 4-*N*-methylaminopyridine **1**, 2-*N*-methylaminopyridine **2**, and 2-*N*,*N*-dimethylaminopyridine **3**, resulted in three novel adducts **1**·2(**I**), **2**·3(**I**), and **3**·3(**I**), one of which **2**·3(**I**) exists in three forms (polymorphs **A**, **B**, **C**). The structure of 2-*N*-methylaminopyridine **2**, that is liquid at room temperature, was also characterized by the single crystal X-ray diffraction analysis. The reasons for the unusual stoichiometry and polymorphic diversity are discussed.

■ EXPERIMENTAL PROCEDURES

General. All initial reagents were purchased from commercial sources and used without further purification. All solvents were of AP-grade. The IR spectra were recorded on a Thermo Nicolet Magna-IR 550 FT-IR spectrometer over the wavenumber range 4000−400 cm^{-1} using the Spectra-Tech Foundation attenuated total reflection (ATR) accessory. Melting points were determined on a Stanford research system (SRS) melting point apparatus and are uncorrected.

The liquid state of **2** and **3** required usage of a considerable excess of 4-nitrophenol in the cocrystallization experiments, as mixing of starting reagents in 1:1, 1:2, and even 1:3 ratios for both pyridine derivatives mostly yielded the gel-like yellow−brown liquids. It is only by repeating experiments with **2** and the triple excess of 4-nitrophenol that we were able to obtain very soft and laminar needle-like crystals which, nevertheless, appeared to be suitable for single crystal X-ray experiment. The structure solution revealed compound **2**·3(**I**), form **A**. Cocrystallization experiments, intended to reproduce polymorph **A**, resulted in a new polymorph, form **B**, whose asymmetric unit comprised two four-membered formula units (Z′ = 2) which are identical to that observed in polymorph **A**. In spite of multiple attempts, we were unable to obtain polymorph **A** again; in all cases polymorph **B** was produced instead. After two months, a few small prism-like crystals were found in the wet bulk material retained after the first crystallization experiment. They have the same composition **2**·3(**I**), but somewhat different crystal structure corresponding to the third polymorph **C**. All polymorphs have very similar crystal shapes and yellow−brown color.

(4-*N*-Methylaminopyridine)·*bis*(4-Nitrophenol), 1·2(I). 4-*N*-Methylaminopyridine (0.5 g, 4.62 mmol) and 4-nitrophenol (1.28g, 9.12 mmol) were dissolved in 10 mL of hot ethanol. The solution was left to cool to room temperature and yellow−brown, block-like crystals were obtained after a few days by slow evaporation. MP = 96 °C. IR, *υ*, cm^{-1}: 3476, 3366, 3224, 2921, 2402, 1633, 1582, 1328, 1271, 1105, 1040, 846, 753, 692.

(2-*N*-Methylaminopyridine)·*tris*(4-Nitrophenol), 2·3(I) (form A). 2-*N*-Methylaminopyridine (0.5 g, 4.62 mmol) and 4-nitrophenol (2.0 g, 14.32 mmol) were dissolved in 15 mL of hot ethanol. The solution was left to cool to room temperature and yellow−brown, block-like crystals were obtained after a few days by slow evaporation. MP = 68−70 °C. IR, *υ*, cm^{-1}: 3404, 3062, 1616, 1571, 1331, 1220, 1164, 1099, 847, 692.

(2-*N*-Methylaminopyridine)·*tris*(4-Nitrophenol), 2·3(I) (form B). 2-*N*-Methylaminopyridine (0.5 g, 4.62 mmol) and 4-nitrophenol (2.0 g, 14.32 mmol) were dissolved in 15 mL of hot ethanol. The solution was left to cool to room temperature and yellow−brown, block-like crystals were obtained after a few days by slow evaporation. MP = 70−71 °C. IR, *υ*, cm^{-1}: 3456, 1647, 1323, 1270, 1125, 1036, 845.

(2-*N*-Methylaminopyridine)·*tris*(4-Nitrophenol), 2·3(I) (form C). A prism-shaped single crystal was selected from the crystals obtained from the first crystallization experiment for 3(**I**)·**2**, (A) after 2 months. MP = 72−74 °C. IR, *υ*, cm^{-1}: 3412, 3058, 1656, 1320, 1220, 1189, 1056, 823.

(2-*N*,*N*-Dimethylaminopyridine)·*tris*(4-Nitrophenol), 3·3(I). 2-*N*,*N*-Dimethylaminopyridine (0.5 g, 3.9 mmol) and 4-nitrophenol (2.0

Table 1. Selected Crystallographic Data for·1·2(I), 2·3(I)· (A, B, C), and 3·3(I)

compound	1·2(I)	2[a]	2·3(I) (A)	2·3(I) (B)	2·3(I) (C)	3·3(I)
formula	$C_{18}H_{18}N_4O_6$	$C_6H_8N_2$	$C_{24}H_{23}N_5O_9$	$C_{24}H_{23}N_5O_9$	$C_{24}H_{23}N_5O_9$	$C_{25}H_{25}N_5O_9$
formula weight	386.36	108.14	525.47	525.47	525.47	539.50
temperature/K	100(2)	143(2)	296(2)	100(2)	100(2)	100(2)
space group	$P2_1/c$	*Pbca*	$P2_1/c$	$P2_1/n$	$P2_1/n$	$P2_1/c$
a/Å	19.836(10)	7.898(3)	10.3822(15)	17.006(4)	7.8501(8)	7.5051(8)
b/ Å	7.193(4)	8.766(3)	14.176(2)	13.708(3)	17.5407(17)	20.064(2)
c /Å	12.924(6)	18.138(8)	17.233(2)	20.859(4)	17.4936(17)	16.9094(17)
β /°	98.587(8)	90	101.212(3)	99.412(3)	102.741(2)	100.157(2).
V/ Å^3	1823.2(15)	1251.0(8)	2487.8(6)	4797.2(18)	2349.5(4)	2506.4(4)
$Z/Z'/Z''$[b]	4/1/3	8/1/1	4/1/4	8/2/8	4/1/4	4/1/4
ρ (calcd)/Mg·m^{-3}	1.408	1.148	1.403	1.455	1.486	1.430
μ/mm^{-1}	0.108	0.072	0.109	0.114	0.116	0.111
reflections collected	16 851	5949	21 176	36 979	19 709	22 411
independent reflections	3568 [R(int) = 0.0659]	947 [R(int) = 0.0528]	4373 [R(int) = 0.0325]	8414 [R(int) = 0.1241]	4627 [R(int) = 0.0223]	4930 [R(int) = 0.0244]
data/restraints/ parameters	3568/0/266	947/0/80	4373/0/360	8414/0/720	4627/0/354	4930/20/401
goodness-of-fit on F^2	1.066	1.030	1.127	1.000	1.011	1.022
final R indices [$I > 2\sigma(I)$]	0.0450, 0.1035	0.0566, 0.1633	0.0685, 0.2016	0.0577, 0.1127	0.0324, 0.0795	0.0340, 0.0879
R indices (all data) R_1, wR_2	0.0738, 0.1179	0.0731, 0.1712	0.0935, 0.2149	0.1267, 0.1381	0.0365, 0.0828	0.0401, 0.0933

[a]Only data obtained at 143 K are included, all three sets (at 273, 203, and 143 K) are deposited in CSD. [b]Z' and Z'' are specified as the number of formula units and the total number of unique molecules in the asymmetric unit, respectively.[26,47]

g, 15.86 mmol) were dissolved in 15 mL of hot ethanol. The solution was left to cool to room temperature and yellow−brown, block-like crystals were obtained after a few days by slow evaporation. MP = 88−92 °C. IR, υ, cm^{-1}: 3256, 3090, 1622, 1596, 1327, 1220, 1165, 849, 751, 693.

In Situ Low-Temperature Crystallization of Compounds 2 and 3. *In situ* low-temperature crystallization of 2-*N*-Methylaminopyridine **2** (m.p. 15 °C) and 2-dimethylaminopyridine **3** (m.p. −70 °C) has been carried out following the procedure reported by us previously.[36] Compounds **2** and **3** each were drawn into a 0.3-mm-diameter Lindemann capillary (∼20 mm length). Capillaries were sealed at both ends with a standard butane burner and attached to a goniometer head, which was mounted on a diffractometer, equipped with a CRYO-FLEX low-temperature device and optical heating crystallization device (OHCD) for laser-assisted crystallization (CO_2 laser, λ = 10.57−10.63 μm). The polycrystalline solids were obtained by freezing at 30 K below melting point. Then, the temperature of solids was elevated up to10 K below melting point. After that, using laser heating (2.0 W laser power), we established solid liquid equilibrium on a narrow zone of the capillary, and crystals were grown by applying the same laser power. The laser power was subsequently reduced to zero over a period of 20 min at the end of the crystallization cycle. After that single crystals were cooled down and X-ray data collection was performed.

X-ray Crystallography. X-ray data collection for single crystals **1**·2(**I**), **2**·3(**I**) (**A**, **B**, **C**), **3**·3(**I**) and **2** was carried out with a Bruker-AXS SMART APEX CCD diffractometer using monochromatized Mo Kα radiation (λ = 0.71073 A) at 273, 203, and 143 K for **2**, at 100 K for **2**·3(**I**) (**B**, **C**) and **3**·3(**I**), and at 295 K for **2**·3(**I**) (**A**). Repeated attempts to find a single crystal of this vanishing polymorph to rerun experiment at low temperature failed so far, so we have at our disposal only RT data for compound **2**·3(**I**) (**A**). Attempts to run the X-ray experiment for the solidified liquid, *N,N*-dimethyl-2-aminopyridine **3**, similar to **2**, failed due to the formation of the glass state for this compound at low temperature. Data reduction and lattice parameters were determined from least-squares analysis, the reflection data were integrated using the program SAINT-Plus,[37] and space groups were determined from systematic absences by XPREP and further justified by refinement results. Semi-empirical absorption corrections were performed on all crystals using SADABS.[38] The structures were solved by direct methods and refined using the Bruker SHELXTL programs suite[39] by full-matrix least-squares methods on F^2 with SHELXL−97. In **2**·3(**I**) (form **C**) the twofold rotation disorder for the *N*-base entity was resolved. The occupancies of these two positions are 0.912(2) and 0.088(2). In **3**·3(**I**) the *N*-base cation **3** is disordered over two positions related by the twofold rotation with the occupancies 0.925(2) and 0.075(2). The soft bond length restraints were applied to the minor component, assuming that the chemically equivalent 1,2- and 1,3-distances were equal in the major and minor disorder components. The non-hydrogen atoms in minor disorder component were refined in the isotropic approximation; the other non-hydrogen atoms in all structures were refined in anisotropic approximation. Aromatic hydrogen atoms were constrained to ride on the parent atoms with C−H = 0.95 Å and Uiso(H) = 1.2 Ueq(C). Methyl hydrogen atoms were constrained to ride on the parent carbon with C−H = 0.98 Å and Uiso(H) = 1.5 Ueq(C) but with free rotation about the C−C bond. The O- and N-bound H atoms were located from the difference Fourier maps and their atomic coordinates and isotropic thermal parameters were refined freely in all structures except the minor components in **2**·3(**I**) (**C**) and **3**·3(**I**), where the N-bound H atoms were refined as riding on the parent N atoms. Structure **2** was refined as a two-block twin with the twinning matrix −1 0 0 0 −1 0 0 0 −1 (BASF = 0.5). Molecular diagrams were produced using SHELXTL,[39] Mercury 3.0,[40] and OLEX2.[41]

■ RESULTS AND DISCUSSION

Two of three *N*-methylaminopyridines used in this study, viz., mono-*N*-methyl-substituted aminopyridines, 4- and 2-*N*-methylaminopyridines (**1** and **2**, Scheme 1) are positional isomers differing by the positions of *N*-methylamino group in the pyridine ring, while in 2-*N,N*-dimethylaminopyridine **3** both hydrogens in amino group are substituted with methyl groups. These variations should obviously result in the different hydrogen bonding systems generating different supramolecular motifs. The liquid state of **2** and **3** is a key factor that impeded their solidification within multicomponent aggregates in conditions reported by us previously,[17] and forced us to use the triple excess of 4-nitrophenol in the reaction mixtures for

Table 2. Hydrogen Bonds for 1·2(I), 2·3(I)·(A, B, C), and 3·3(I) [Å and °]

D—H···A	d(D—H)	d(H···A)	d(D···A)	∠(DHA)	symmetry transformation for acceptor
			1·2(I)		
O(3)−H(3)···O(4)	1.06(3)	1.47(3)	2.518(2)	169(3)	*x, y, z*
N(1)−H(1)···O(4)	1.02(3)	1.67(3)	2.663(3)	163(2)	*x, y, z*
N(2)−H(2)···O(2)	0.88(3)	2.34(3)	3.132(3)	149(3)	1−*x*, *y*+1/2, 1/2−*z*
N(2)−H(2)···O(1)	0.88(3)	2.57(3)	3.411(3)	159(3)	1−*x*, *y*+1/2, 1/2−*z*
			2·3(I) (A)		
O(3)−H(3A)···O(4)	1.00(4)	1.59(5)	2.568(3)	167(4)	*x, y, z*
O(9)−H(9A)···O(4)	0.92(4)	1.64(4)	2.552(3)	174(4)	*x, y, z*
N(1)−H(1)···O(5)	0.78(4)	2.09(4)	2.869(4)	173(4)	*x, y, z*
N(2)−H(2)···O(6)	0.84(5)	2.26(6)	3.074(4)	162(5)	*x, y, z*
			2·3(I) (B)		
O(6)−H(1O)···O(3)	1.05(4)	1.50(4)	2.543(3)	175(3)	*x, y, z*
O(9)−H(2O)···O(18)	1.04(5)	1.55(5)	2.565(3)	164(4)	1−*x*, 1−*y*, −*z*
O(12)−H(3O)···O(18)	1.00(4)	1.59(4)	2.576(3)	170(3)	1−*x*, 1−*y*, −*z*
N(1)−H(1N)···O(1)	0.97(4)	2.28(4)	3.198(4)	159(3)	3/2−*x*, *y*+1/2, 1/2−*z*
N(2)−H(2N)···O(2)	0.90(4)	1.94(5)	2.821(4)	168(4)	3/2−*x*, *y*+1/2, 1/2−*z*
N(3)−H(3N)···O(17)	1.01(4)	1.87(4)	2.876(4)	173(3)	*x, y, z*
N(4)−H(4N)···O(16)	0.84(3)	2.11(4)	2.927(4)	163(3)	*x, y, z*
O(15)−H(4O)···O(3)	0.96(5)	1.62(5)	2.572(3)	172(5)	*x, y, z*
			2·3(I) (C)		
O(3)−H(1O3)···O(4)	0.93(2)	1.62(2)	2.5496(13)	179(2)	*x, y, z*
O(9)−H(1O9)···O(4)	0.90(2)	1.69(2)	2.570(1)	166(2)	*x*+1, *y*, *z*
N(1)−H(1N)···O(5)	0.89(2)	2.02(2)	2.900(2)	168(2)	*x*−1, *y*, *z*
N(2)−H(2N)···O(1)	0.85(2)	2.20(2)	2.962(2)	150(2)	*x*, *y*, *z*+1
			3·3(I)		
O(6)−H(6)···O(1)	0.90(2)	1.66(2)	2.557(1)	170(2)	*x, y, z*
O(7)−H(7)···O(1)	0.95(2)	1.59(2)	2.542(1)	176(2)	*x, y, z*
N(1)−H(1)···O(5)	0.86	2.01	2.843(2)	164	*x, y, z*
N(1)−H(1)···O(5)	0.86	1.97	2.748(12)	150	*x, y, z*

successful cocrystallization. As reported in the Experimental section, compound **2**·3(**I**) exists as three polymorphs **A**, **B**, and **C**. Experimental observations show that polymorphs **B** and **C** are the predominant forms, while the crystalline form **A** was impossible to reproduce and we consider it to be vanishing polymorph[33] similar to the one previously reported by us for (2*E*)-2-cyano-3-[4-(diethylamino)phenyl]prop-2-enethioamide.[42] The X-ray data provide evidence for the proton transfer from phenoxy group to pyridine nitrogen and salt formation in all adducts. Selected crystallographic data for **1**·2(**I**), **2**, **2**·3(**I**) (**A**, **B**, **C**), and **3**·3(**I**) are summarized in Table 1. The selected H-bond geometric characteristics for all compounds are presented in Table 2.

Compound **1**·2(**I**) crystallizes in the monoclinic centrosymmetric space group $P2_1/c$; the asymmetric unit comprises pyridinium cation, 4-nitrophenolate anion, and neutral 4-nitrophenol molecule (Figure 1a). The structure of the H-bonded trimer looks like the similar adducts of aminopyridines reported so far,[14−17] being composed of the H-bonded slightly twisted 4-nitrophenol-4-nitrophenolate entity (the dihedral angle between the mean planes of the molecules is 20.88(5)°) and the pyridinium cation anchored to it. The dihedral angle between the cation's and anion's mean planes is equal to 55.89(5)°. The shortest H-bonds within the trimer include the OH···O$^-$ hydrogen bond, O(3)···O(4) 2.513(3) Å in the 4-nitrophenol-4-nitrophenolate anionic dimeric scaffold, and NH$^+$···O$^-$ hydrogen bond, N(1)···O(4) 2.662(3) Å between the pyridinium cation and nitrophenolate anion. The next in strength NH···O bifurcated hydrogen bond between the NHMe group as H-donor and nitro group as H-acceptor (Table 2) links the adjacent formula units related by the twofold screw axis, thus generating the helical chains (Figure 1b), where the anionic scaffold and the cation of the next trimeric unit are almost coplanar as the cation/neutral molecule and cation/anion dihedral angles [6.53(8)° and 14.35(6)°, respectively] indicate. The helical pitch of 7.193(4) Å allows fitting a second helix (Figure 1c,d) providing the parallel arrangement of the related by the inversion center trimeric entities (cation−neutral molecule−anion) that belong to the adjacent helices (Figure 1e). The interplanar separation between their mean planes is 3.39 Å; the overlapping pattern is shown in Figure 1e.

2-*N*-Methylaminopyridine **2**, the positional isomer of 4-*N*-methylaminopyridine, is a liquid at ambient conditions, MP 15 °C. With the miniature zone melting *in situ* crystallization technique,[36] the crystal of 2-*N*-methylaminopyridine was grown, and its molecular and crystal structures were determined at 273, 203, and 143 K. 2-*N*-Methylaminopyridine crystallizes in the orthorhombic space group *Pbca*, Z' = 1. At all temperatures the H atom of the secondary amino group and the pyridine nitrogen are in distal *anti*-position, as the torsion angle H(4)−N(4)−C(2)−N(1) of −173(2)° indicates. Such a conformation is most likely stabilized by the involvement of amino group and pyridine nitrogen in the NH···N hydrogen bond, N(4)−H(4)···N(1)(1/2−*x*, *y*+1/2, *z*) 2.25(3), 3.048(4) Å, ∠NHN 169(3)°, that leads to the chain structure (Figure 2). The endocyclic angles in pyridine ring cover the range 117.12(5)−124.24(5)°. The endocyclic angles at the carbon atoms adjacent to the N(1) heteroatom are larger than 120°, and those at the other atoms of the ring are smaller than 120°.

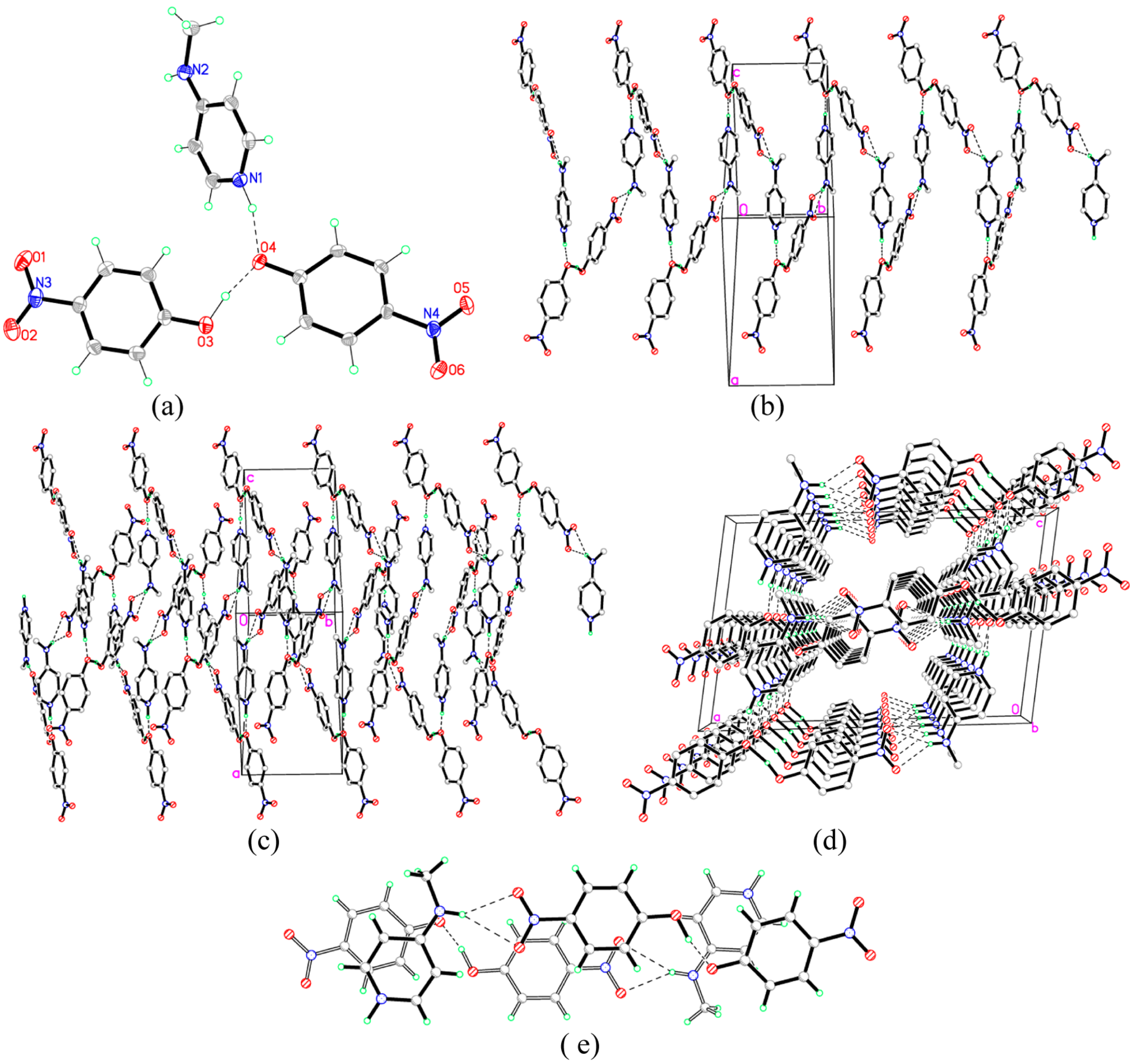

Figure 1. (a) Asymmetric unit of **1**·2(**I**) with partial numbering scheme. Thermal ellipsoids are shown at the 50% probability level. (b) View of the helical chain in **1**·2(**I**). C-bound H atoms are omitted for clarity. (c,d) Interdigitation of two helical chains: (c) view along the diagonal of the *ac* plane; (d) view along the *b* axis. (e) Stacking mode of flattened H-bonded entities belonging to the adjacent helices in projection on the entity shown by open lines.

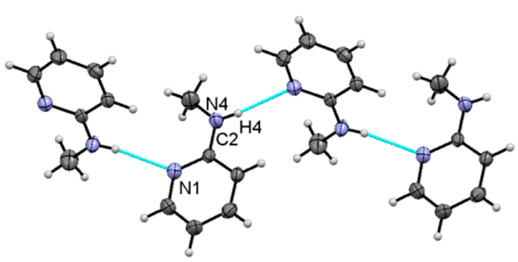

Figure 2. Fragment of H-bonded chain in the crystal structure of **2**.

The same distribution of endocyclic angles was observed in the molecules of similar pyridine compounds reported by us earlier.[43]

Compound **2**·3(**I**)·(**A**, **B**, **C**) crystallizes from ethanol solution as three one-pot polymorphs (forms **A**, **B**, and **C**), thus presenting an example of concomitant polymorphism.[44−46] All polymorphic forms belong to the monoclinic crystal system, and crystallize in what is essentially the same centrosymmetric space group No. 14, which is set as $P2_1/c$ in **A**, and $P2_1/n$ in **B** and **C** (Table 1). The formula units are shown in Figure 3. The unit cell volume for form **B** is approximately twice as big as those for forms **A** and **C**. In the smaller unit cells **A** and **C** the asymmetric units comprise one formula unit each that includes 2-*N*-methylaminopyridinium cation, one 4-nitrophenolate anion, and two neutral 4-nitrophenol molecules held together via hydrogen bonding, thus revealing $Z' = 1$ and $Z'' = 4$ (calculated as a number of unique molecules in the asymmetric unit)[47] in both cases. The asymmetric unit for polymorph **B** comprises two such aggregates, i.e., two cations, two anions, and four neutral molecules thus revealing $Z' = 2$ and $Z'' = 8$ (Figure 3b). The 1:3 molar ratio is common for three polymorphs and differs from the 1:1 and 1:2 stoichiometries for the similar solids previously reported.[17] To the best of our knowledge such a ratio for adducts with 4-

dx.doi.org/10.1021/cg500360f | Cryst. Growth Des. 2014, 14, 3423−3433

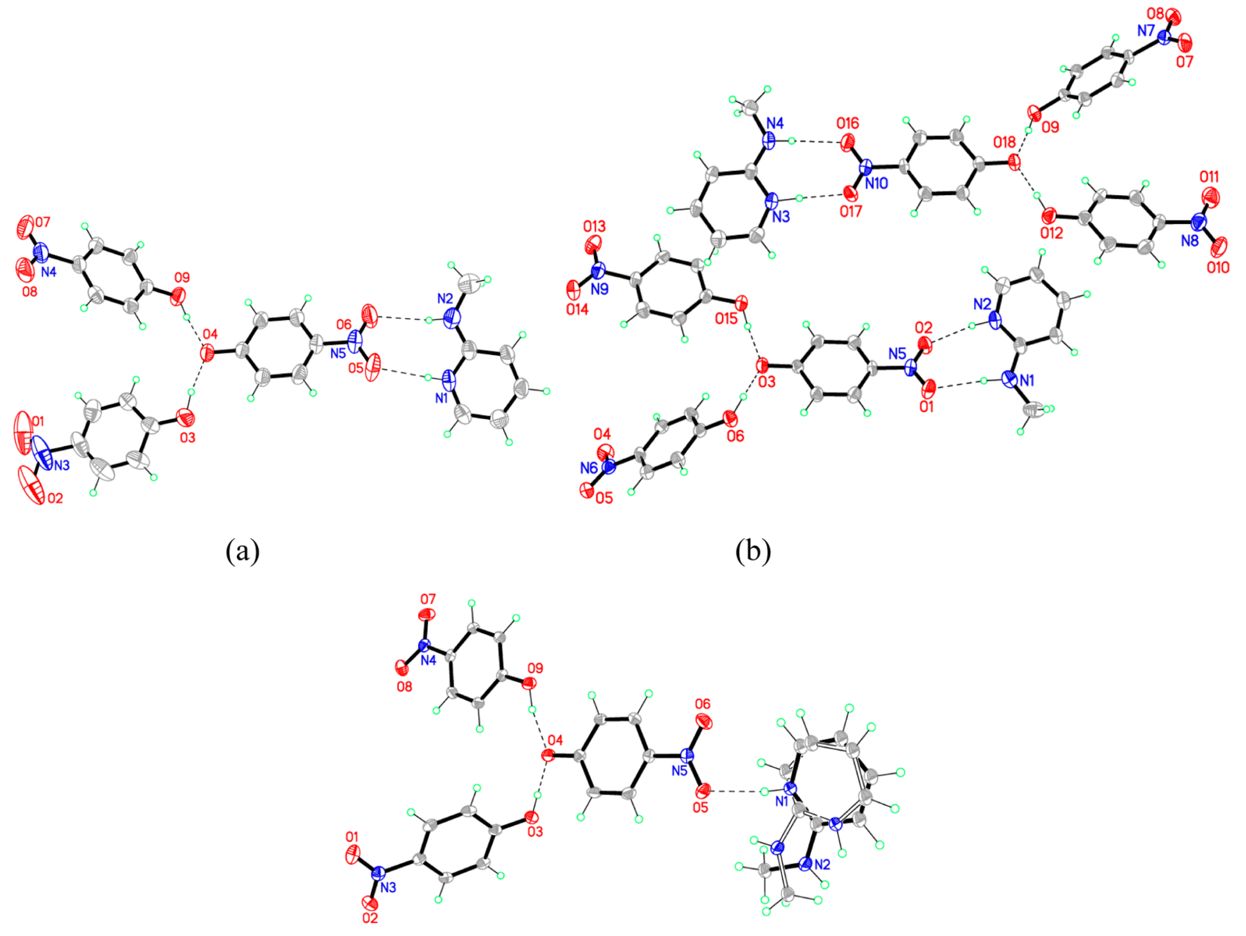

Figure 3. Asymmetric units for polymorphs **2**·3(**I**) with partial numbering schemes. (a) Form **A**: thermal ellipsoids are drawn at the 30% probability level. (b) Form **B**: thermal ellipsoids are drawn at the 50% probability level. (c) Form **C**: thermal ellipsoids are drawn at the 50% probability level. The minor component of the disordered *N*-base cation is indicated by open lines.

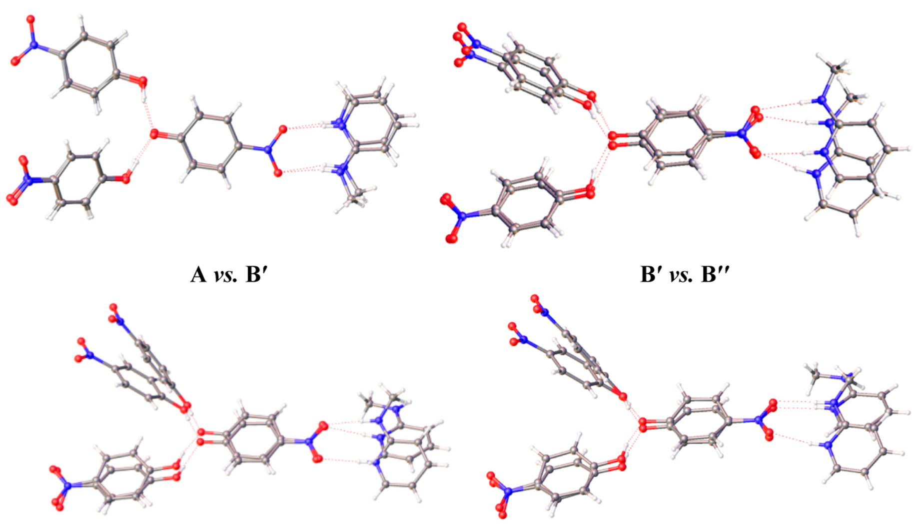

Figure 4. Overlapping diagrams for three polymorphs **2**·3(**I**).

nitrophenol has been reported only once for the cocrystal with L-tryptophan, viz., (L-tryptophan)(*tris*-4-nitrophenol).[48]

A common feature for all three polymorphs is the mode of self-association of three 4-nitrophenol moieties. The two neutral molecules and its anionic conjugate are held together via a couple of the shortest OH···O⁻ hydrogen bonds, O···O being in the range 2.543(3)–2.576(3) Å (Table 2). As evidenced from the inspection of the overlapping diagrams

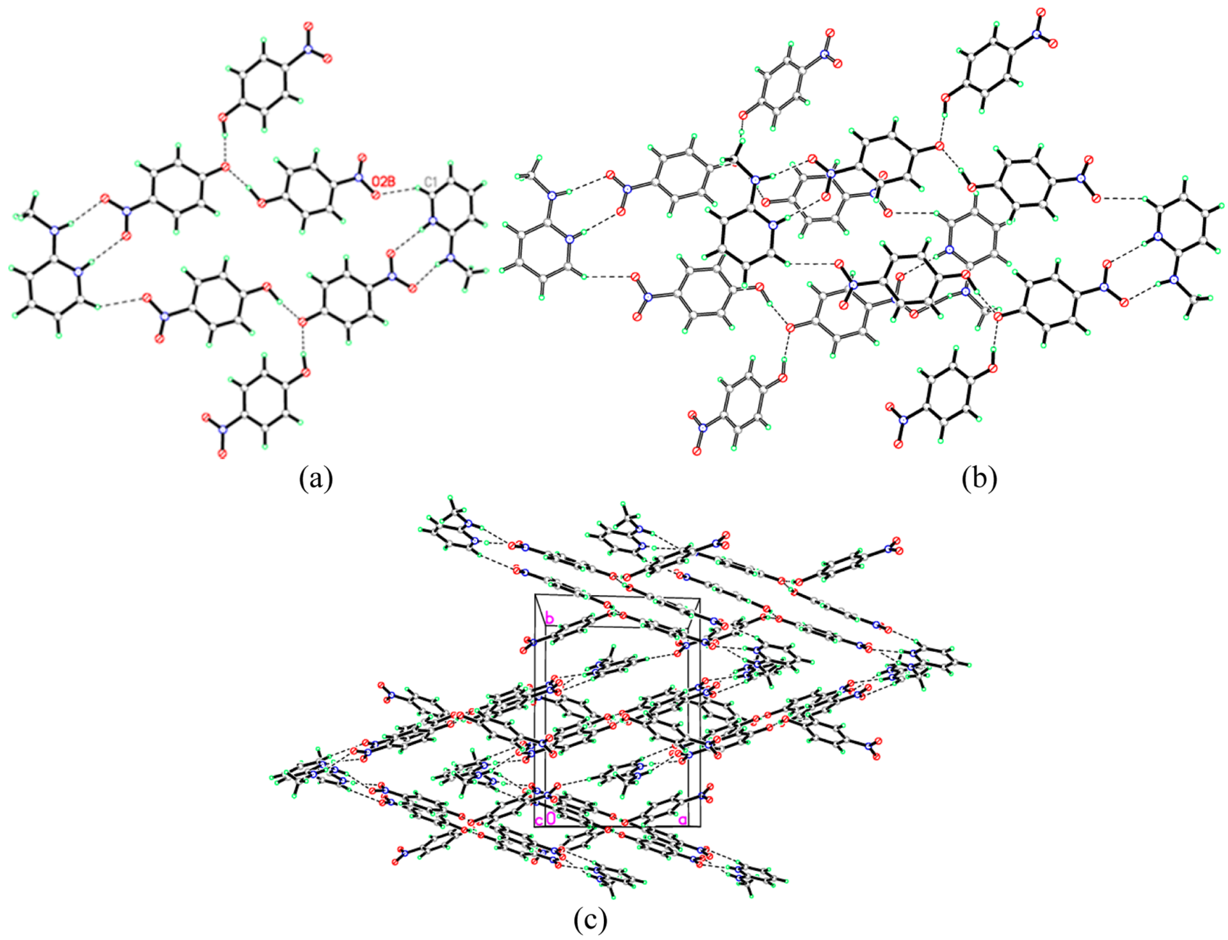

Figure 5. Fragments of crystal packing in **2**·3(**I**), polymorph **A**. (a) Association of two formula units in the centrosymmetric cluster. Labeled are atoms that participate in the CH···O hydrogen bond, symmetry transformation B: 1−*x*, 1−*y*, 1−*z*. (b) Mode of overlap in the offset stack in projection of the molecules shown by open lines. (c) Herringbone packing mode.

depicted in Figure 4, polymorphs differ by (a) the topology of H-bonded pattern within the three-membered homomeric associate, (b) the conformation of the *N*-base cation, and (c) the heteromeric H-bonded patterns. Similar to 2(**I**)·**1** and other adducts of 4-nitrophenol with the 2:1 ratio, two nitrophenol moieties form the slightly twisted anionic scaffold with the dihedral angle between the mean planes of the molecules equal to 4.7(1)° in polymorph **A**, 9.25(5)/11.12(5)° in two formula units (**B**′/**B**″) in polymorph **B**, and 5.06(2)° in polymorph **C**. The second 4-nitrophenol neutral molecule is attached to the anion in an angular mode as the dihedral angles between the mean planes of the molecules equal to 44.14(6)° in **A**, 36.31(6)/45.53(5)° in **B**′/**B**″, and 68.89(2)° in **C** indicate. These quantitative characteristics describing the 4-nitrophenol trimers correlate with the overlapping diagrams (Figure 4). The pair **A** vs **B**′ (Figure 4a) reveals better fitting than the same two entities in two formula units of polymorph **B** (Figure 4b), while an essential discrepancy is observed in the pairs **B**″ vs **C** and **A** vs **C** (Figure 4c,d). The conformation of 2-*N*-methylpyridinium cation **2** in polymorphs **A** and **B** differs from that of polymorph **C**. Contrary to the *anti*-conformer observed in the *N*-base pure form (Figure 2), in polymorphs **A** and **B** the pyridinium cation **2** exists as *syn*-conformer due to its chelate involvement in two NH···O hydrogen bonds which give rise to the cyclic asymmetric $R_2^2(8)$ hydrogen bonding patterns[49] (Figures 3, 4, Table 2). Again, we observe quite nice fitting of the heteromeric cation/anion aggregates linked by this pattern in the pair **A** vs **B**′; the fitting is getting worse in **B**′ vs **B**″, being almost in line with the values of the cation/anion dihedral angles of 27.59(7)° in **A**, 14.85(9)° and 27.43(6)° in **B**′ and **B**″. The formula units **B**′ and **B**″ differ by the degrees of twisting both within the homomeric anionic component and within the acid−base $R_2^2(8)$ H-bonded fragments.

As follows from the different modes of aggregation of molecular species within the formula units in three polymorphs, the next in hierarchy association patterns should also differ, and it was observed through analysis of crystal packings. In form **A** two formula units are combined into centrosymmetric cluster via two C(1)H···O(2)(NO_2) hydrogen bonds [C···O 3.313(5), H···O 2.50 Å, ∠CHO 146.6°], with 6 of 8 molecules being arranged approximately in the same plane (Figure 5a). These clusters form face-to-face offset stacks (Figure 5b), being packed in a herringbone mode along the (1 1 0) and (1 −1 0) directions (Figure 5c). The interplanar separation between the neighboring clusters in the stack is 3.46 Å; the mode of overlapping within the stack is shown in Figure 5b.

In polymorph **B** two formula units **B**′ and **B**″ form different self-association patterns: units **B**′ are dimerized into centrosymmetric clusters identical to form **A** [C···O 3.228(5), H···O 2.32 Å, ∠CHO 164.8°] (Figure 6a), while units **B**″ are aggregated into zigzag chains via CH(Me)···O hydrogen bond with participation of CH(Me) hydrogen atom and the lone pair of the phenolic hydroxyl [C···O 3.391(5), H···O 2.55 Å, ∠CHO 146.0°] (Figure 6b). The dimeric clusters are

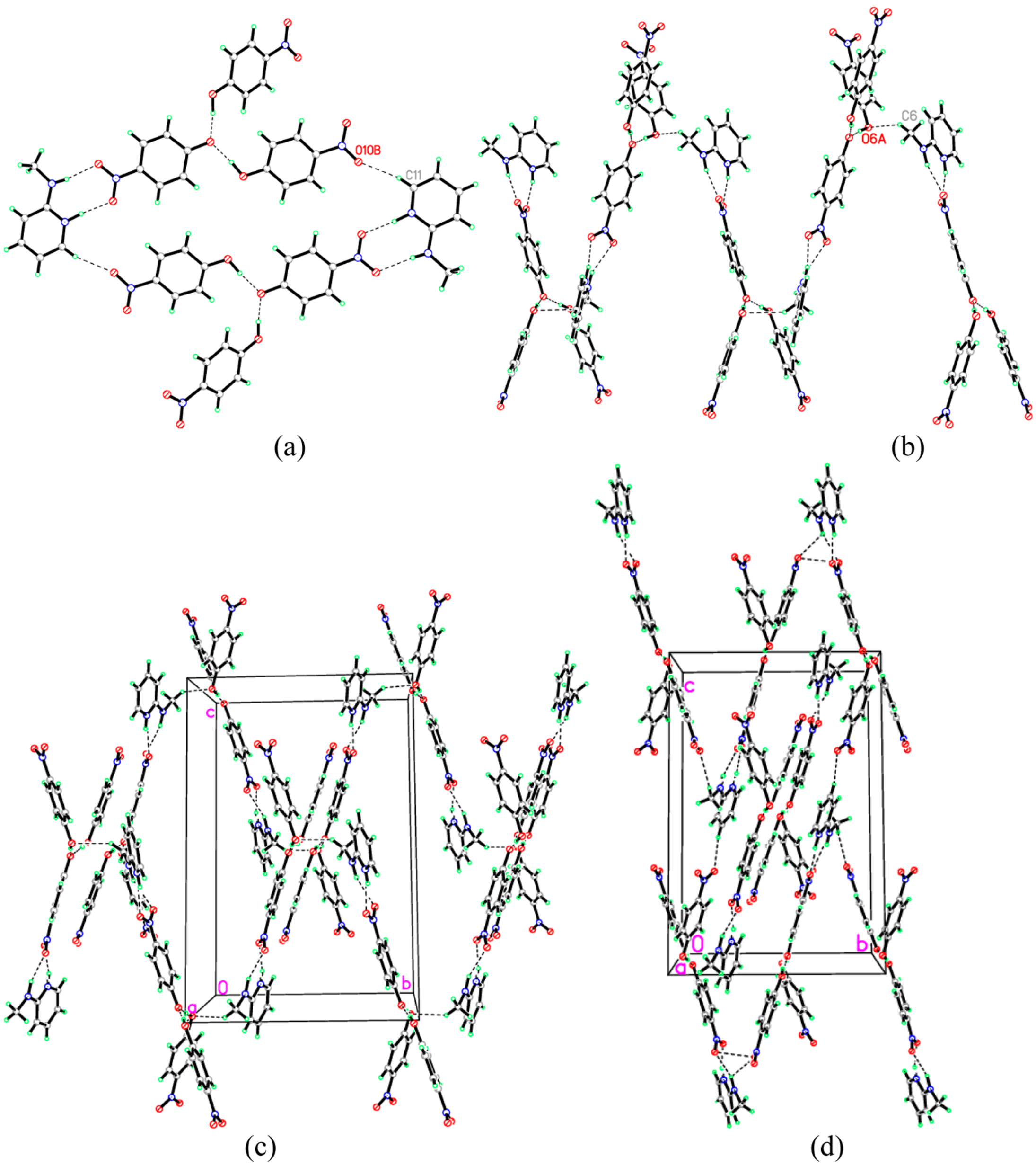

Figure 6. Fragments of crystal packing in **2**·3(**I**), polymorph **B**. (a) Association of two formula units **B**′ in the centrosymmetric cluster. Labeled are atoms that participate in the CH⋯O hydrogen bond, symmetry transformation B: 1−*x*, 1−*y*, −*z*. (b) Association of formula units **B**″ in the zigzag chain. Labeled are atoms that participate in the CH⋯O hydrogen bond, symmetry transformation A: 3/2−*x*, *y*−1/2, 1/2−*z*. (c) View of two centrosymmetric zigzag chains. Cluster 2·(**B**′) is omitted for clarity. (d) Mode of accommodation of cluster 2·(**B**′) in the crystal lattice.

accumulated in the voids provided by the packing of zigzag chains (Figure 6c,d). Thus, forms **A** and **B** support the cited above statement about the possibility of multivariant superposition of the similar supramolecular fragments in polymorphs.[13]

Meanwhile, in polymorph **C** the pyridinium cation adopts the same *anti*-conformation as in the crystal of individual compound **2** that is justified by the same involvement in the H-bonded chains via two hydrogen bonds (Figures 2, 7a). The staircase-like chains with interplanar separation of 6.75 Å between the neighboring planar segments linked by the bridging 4-nitrophenol molecule allow adjusting the next chains with the parallel alignment of the aromatic units (Figure 7b), giving rise to the most effective crystal packing among three polymorphic forms.

Thus, three polymorphs of **2**·3(**I**) give an example of synthon polymorphism[50−52] since the cyclic cation−anion H-bonded pattern found in forms **A** and **B** is transformed to the single H-bond in form **C**. Three polymorphs differ by the unit cell volumes, melting points, crystal densities, and packing indices[53] (Table 3). The comparison of all these parameters shows that form **C** has the smallest unit cell volume and the highest crystal density which is often an indication of the highest stability.[54]

Compound 3·3(I). Given the composition and structure of three polymorphs **2**·3(**I**), the structure of the adduct **3**·3(**I**) with 1:3 molar ratio looks by no means unexpected, especially taking into account the liquid nature of the starting base, 2-*N,N*-dimethylaminopyridine **3**, and the crystallization conditions which are practically identical to those used for **2**·3(**I**). The view of formula unit for **3**·3(**I**) is shown in Figure 8a. Three strong H-bonds (Table 2) within the tetramer provide

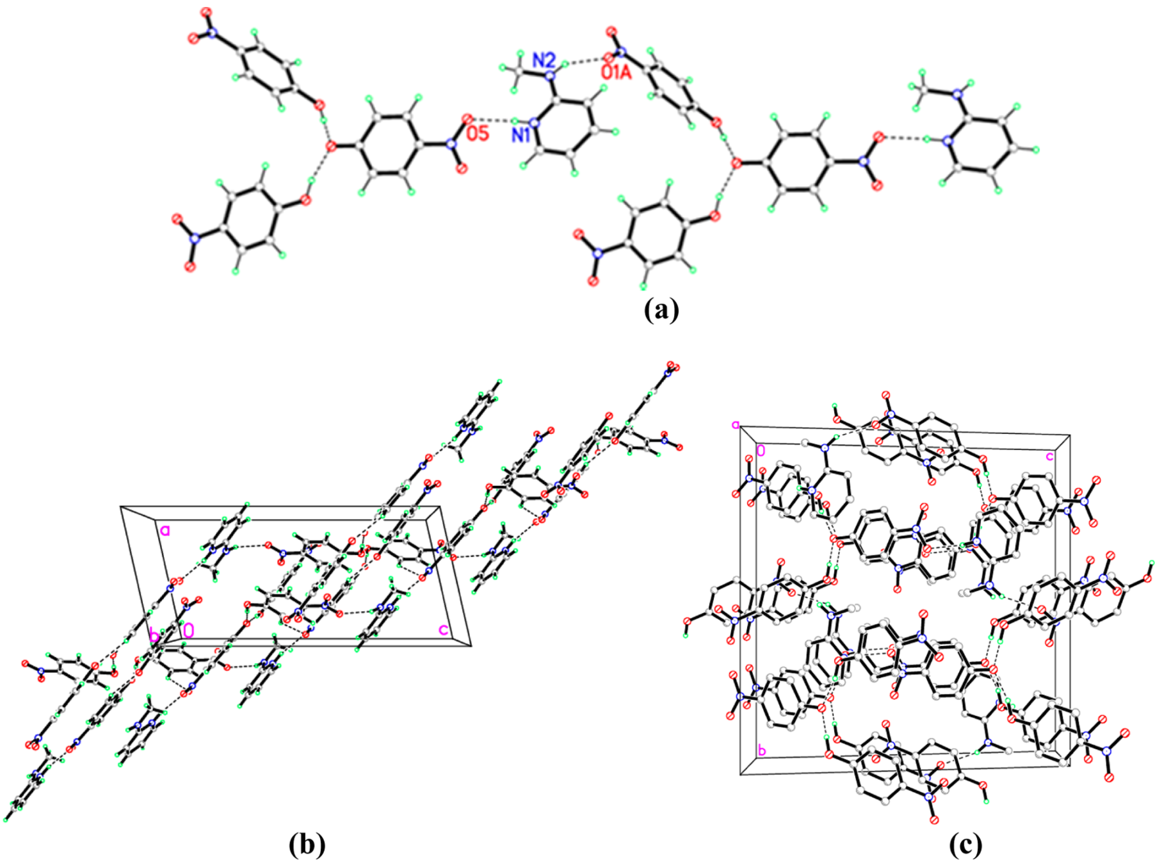

Figure 7. Fragments of crystal packing in polymorphs **2**·3(**I**). (a) H-bonded chain in form C. Labeled are atoms that participate in H-bonds, symmetry transformation A: *x*, *y*, 1+*z*. (b) Packing of the chains. H-bonds are shown by dashed lines. (c) Mode of intermolecular stacking. The C-bound H atoms are omitted for clarity.

Table 3. Selected Characteristics for Polymorphic Landscape 2·3(I)· (A, B, C), and 3·3(I)

compound	**2**·3(I) (A)	**2**·3(I) (B)	**2**·3(I) (C)	**3**·3(I)
m.p./°C	68–70	71.5	72–74	88–92
V^a/ Å^3	2487.8(6)	4797.2(18)	2349.5(4)	2506.4(4)
ρ (calcd)/Mg·m^{-3}	1.403	1.455	1.486	1.430
PI^b	68.4	71.4	73.3	70.9

^{a}Volume of crystal unit cell. ^{b}Kitajgorodskij Packing Index.[53]

an almost coplanar arrangement of three entities, 4-nitrophenol neutral molecule, 4-nitrophenolate anion, and 2-*N*,*N*-dimethylaminopyridinium cation, as the dihedral angles of 8.04(4)° and 8.06(6)° in the pairs neutral molecule/anion and anion/cation indicate. The second neutral 4-nitrophenol molecule attached to the anionic component of this slightly corrugated scaffold is inclined to the anion (the dihedral angle between the mean planes of the molecules is 46.15(2)°). The crystal packing is additionally governed by CH···O hydrogen bonds [C···O 3.254(2), H···O 2.45 Å, ∠CHO 144.7°] combining the formula units into the centrosymmetric clusters (Figure 8b) and stacking interactions between the extended planar entities that align in the crystal parallel to the (2 2 1) and (−2 2 1) planes with the interplanar separation of 3.48 Å (Figure 8c).

The similarities in starting materials, crystallization conditions, molecular structures, and crystal packings allow fitting the three polymorphs of **2**·3(**I**) and the **3**·3(**I**) adduct within the common structural landscape,[51] considering the last compound as a conformational pseudo polymorph of polymorph **C**.

Thus, the cocrystallization of 4-nitrophenol with *N*-methyl-substituted aminopyridines resulted in three crystalline solids (one in three polymorphic forms) with 1:2 and 1:3 molar ratio. The components in the formula units are held together via charge-assisted OH···O$^-$ and NH$^+$···O$^-$ hydrogen bonds. All structures reveal the hydrophilic regions[55] that accumulate two or three 4-nitrophenol−4-nitrophenolate entities associated through one or two single OH···O$^-$ hydrogen bonds. Because these adducts enrich the statistics for the systems containing the H-bonded 4-nitrophenol-4-nitrophenolate entity,[6,14−17] we may consider it (in line with the suggestions for the neutral OH···O synthon registered in the diols[55,56]) as a robust supramolecular synthon generated in the heteromolecular systems in the presence of N-aromatic base. Contrary to the previously reported (by us) adducts between aminopyridines and 4-nitrophenol with 1:1 and 1:2 molar ratio that crystallize in the acentric space groups $P2_1$ and $Pna2_1$,[17] all solids reported herein represent the centrosymmetric crystals. The reason we see the "weakening" of helicity that is suppressed by two events, viz., incorporation of methyl groups in the primarily amino

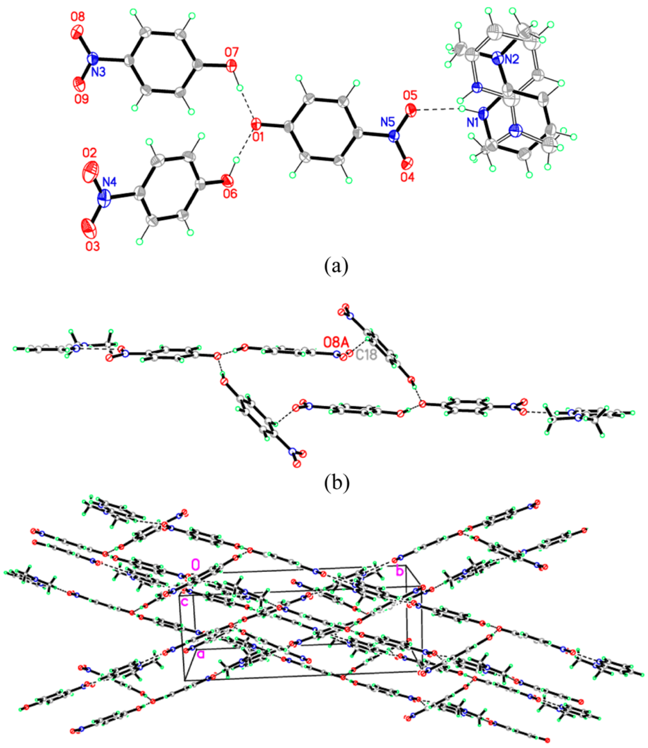

Figure 8. (a) Asymmetric unit for **3**·3(**I**). Thermal ellipsoids are shown at the 50% probability level. The minor component of the disordered *N*-base cation is indicated by open lines. (b) Centrosymmetric cluster generated via CH···O hydrogen bonds. Labeled are atoms that participate in H-bonds, symmetry transformation A: 1−*x*, 1−*y*, 1−*z*. (c) Slice of the crystal packing showing fragments of stacks of H-bonded ribbons aligned parallel to the (2 2 1) and (−2 2 1) planes. View along the *c* axis.

group, and increased amount of 4-nitrophenol molecules in the systems. The first event reduces the number of strong H-donors in the N-bases. Their deficiency explains the involvement of CH-groups in the structurally meaningful hydrogen bonds[57−59] that often act across inversion centers and combine the extended formula units in the centrosymmetric arrays. The concerted contribution of both events results in the planarity enhancement in the systems, achieved via planarization of the *N*-methyl-substituted amino group, and creation of the extended planar arrays composed of the neutral and charged species, the latter ones reinforcing the stacking interactions.[60,61] The more planar the system is, the stronger stacking interactions, the farther the system is from helicity and acentricity.

CONCLUSION

Four new adducts of 4-nitrophenol with *N*-methylaminopyridines, 4-*N*-methylaminopyridine, 2-*N*-methylaminopyridine, and 2-*N,N*-dimethylaminopyridine have been obtained and their crystal and molecular structures were determined and analyzed. The cocrystallization experiments with liquid 2-*N*-methylaminopyridine and 2-*N,N*-dimethylaminopyridine resulted in adducts with unusual 1:3 molar ratio necessary to compensate the differences in solubilities of starting materials. To the best of our knowledge the only example of 1:3 stoichiometry for cocrystals involving 4-nitrophenol, viz., (L-tryptophan)(*tris*-4-nitrophenol) has been reported so far.[46] Contrary to the previously reported (by us) acentric adducts between 4-nitrophenol and aminopyridines,[17] all new compounds crystallize in the centrosymmetric space group. The reason for what we see in the reduced number of strong H-donors, and even though the stable acentric supramolecular synthons[13] are realized within the trimeric and tetrameric formula units, the weaker hydrogen bonds and stacking interactions control the centrosymmetric packing. The one-pot cocrystallization resulted in three polymorphs for adduct (2-*N*-methylaminopyridinium)(4-nitrophenolate)*bis*(4-nitrophenol), which offers an example of conformational polymorphism,[32−34] originated in the intramolecular rotation of *N*-methyl amino group in the 2-*N*-methylaminopyridinium cation. The discovery of 3 + 1 polymorphs for the multicomponent systems comprising pyridinium cations similar in composition, 4-nitrophenolate anion, and 4-nitrophenol neutral molecules, along with other recent examples,[31,62−67] indicates the possibility of polymorphic diversity in the supramolecular systems.

ASSOCIATED CONTENT

Supporting Information

Precession images and crystallographic information files (cif) for all compounds. This material is available free of charge via the Internet at http://pubs.acs.org. Crystallographic data for new structures reported herein were deposited with the Cambridge Crystallographic Data Centre and allocated the deposition numbers CCDC 991678−991685. These data can be obtained free of charge from the Cambridge Crystallographic Data Centre via www.ccdc.cam.ac.uk/data_request/cif.

AUTHOR INFORMATION

Corresponding Author

*E-mail: sergiudraguta@gmail.com.

Notes

The authors declare no competing financial interest.

ACKNOWLEDGMENTS

The advice of the anonymous reviewers is acknowledged. The authors are grateful for NSF support via DMR-0934212 (PREM) and IIA-130134.

DEDICATION

Dedicated to the memory of Professor M. Yu. Antipin.

REFERENCES

(1) Childs, S. L.; Zaworotko, M. J. *Cryst. Growth Des.* **2009**, *9*, 4208−4211.
(2) Hickey, M. B.; Peterson, M. L.; Scoppettuolo, L. A.; Morrisette, S. L.; Vetter, A.; Guzman, H.; Remenar, J. F.; Zhang, Z.; Tawa, M. D.; Haley, S.; Zaworotko, M. J.; Almarsson, O. *Eur. J. Pharm. Biopharm.* **2007**, *67*, 112−119.
(3) Caira, M. R. *Mol. Pharmaceutics* **2007**, *4*, 310−316.
(4) Marder, S. R.; Perry, J. W.; Yakymyshyn, C. P. *Chem. Mater.* **1994**, *6*, 1137−1147.
(5) Pan, F.; Wong, M. S.; Bosshard, C.; Günter, P. *Adv. Mater.* **1996**, *8*, 592−595.
(6) Evans, C. C.; Bagieu-Beucher, M.; Masse, R.; Nicoud, J.-F. *Chem. Mater.* **1998**, *10*, 847−854.
(7) Etter, M. C. *J. Phys. Chem.* **1991**, *95*, 4601−4610.
(8) Gavezzotti, A.; Filippini, G. *J. Am. Chem. Soc.* **1995**, *117*, 12299−12305.
(9) Brock, C. P.; Dunitz, J. D. *Chem. Mater.* **1994**, *6*, 1118−1127.

(10) Kelley, S. P.; Fabian, L.; Brock, C. P. *Acta Crystallogr.* **2011**, *B67*, 79−93.
(11) Kuleshova, L. N.; Antipin, M. Yu. *Crystallogr. Rep.* **2002**, *47*, 268−280.
(12) Kuleshova, L. N.; Antipin, M. Yu. *Crystallogr. Rep.* **2003**, *48*, 259−279.
(13) Hofmann, D. W. M.; Kuleshova, L. N.; Antipin, M. Yu. *Cryst. Growth Des.* **2004**, *4*, 1395−1402.
(14) Prakash, M. J.; Radhakrishnan, T. P. *Cryst. Growth Des.* **2005**, *5*, 721−725.
(15) Anandha babu, G.; Ramasamy, R. P.; Ramasamy, P. *Mater. Chem. Phys.* **2009**, *117*, 326−330.
(16) Chen, T.; Sun, Z.; Li, L.; Wang, S.; Wang, Y.; Luo, J.; Hong, M. *J. Cryst. Growth* **2012**, *338*, 157−161.
(17) Draguta, S.; Fonari, M. S.; Masunov, A. E.; Zazueta, J.; Sullivan, S.; Antipin, M. Yu.; Timofeeva, T. V. *CrystEngComm* **2013**, *15*, 4700−4710.
(18) Aher, S.; Dhumal, R.; Mahadik, K.; Paradkar, A.; York, P. *Eur. J. Pharmaceut. Sci.* **2010**, *41*, 597−602.
(19) Lemmerer, A.; Fernandes, M. A. *New J. Chem.* **2012**, *36*, 2242−2252.
(20) Luo, Y.-H.; Zhang, C.-G.; Xu, B.; Sun, B.-W. *CrystEngComm* **2012**, *14*, 6860−6868.
(21) Morissette, S. L.; Almarsson, Ö.; Peterson, M. L.; Remenar, J. F.; Read, M. J.; Lemmo, A. V.; Ellis, S.; Cima, M. J.; Gardner, C. R. *Adv. Drug Delivery Rev.* **2004**, *56*, 275−300.
(22) Fleischman, S. G.; Kuduva, S. S.; McMahon, J. A.; Moulton, B.; Walsh, R. D. B.; Rodríguez-Hornedo, N.; Zaworotko, M. J. *Cryst. Growth Des.* **2003**, *3*, 909−919.
(23) McKellar, S. C.; Kennedy, A. R.; McCloy, N. C.; McBride, E.; Florence, A. J. *Cryst. Growth Des.* **2014**, *14*, 2422−2430.
(24) Lirag, R. C.; Osowska, K.; Miljanić, O. Š. *Org. Biomol. Chem.* **2012**, *10*, 4847−4850.
(25) Aitipamula, S.; Chow, P. S.; Tan, R. B. H. *CrystEngComm* **2009**, *11*, 1823−1827.
(26) Steed, J. W. *CrystEngComm* **2003**, *5*, 169−179.
(27) Anderson, K. M.; Goeta, A. E.; Martin, J. E.; Mason, S. A.; McIntyre, G. J.; Sansam, B. C.R.; Wilkinson, C.; Steed, J. W. *Cryst. Growth Des.* **2011**, *11*, 4904−4919.
(28) Trask, A. V.; van de Streek, J.; Motherwell, W. D. S.; Jones, W. *Cryst. Growth Des.* **2005**, *5*, 2233−2241.
(29) Day, G. M.; Motherwell, W. D. S.; Jones, W. *Cryst. Growth. Des.* **2005**, *5*, 1023−1033.
(30) Jayasankar, A.; Sreenivas Reddy, L.; Bethune, S. J.; Rodriguez-Hornedo, N. *Cryst. Growth Des.* **2009**, *9*, 889−897.
(31) Eddleston, M. D.; Patel, B.; Day, G. M.; Jones, W. *Cryst. Growth Des.* **2013**, *13*, 4599−4606.
(32) Nangia, A. *Acc. Chem. Res.* **2008**, *41*, 595−604.
(33) (a) Bernstein, J. *Polymorphism in Molecular Crystals*; Oxford Science Publications: Oxford, 2002. (b) Cruz-Cabeza, A. J.; Bernstein, J. *Chem. Rev.* **2014**, *114*, 2170−2191.
(34) Bauer, J.; Spanton, S.; Henry, R.; Quick, J.; Dziki, W.; Porter, W.; Morris, J. *Pharm. Res.* **2001**, *18*, 859−866.
(35) Suzuki, M.; Kobayashi, K. *Cryst. Growth Des.* **2011**, *11*, 1814−1820.
(36) Yakovenko, A. A.; Gallegos, J. H.; Antipin, M. Yu.; Masunov, A.; Timofeeva, T. V. *Cryst. Growth Des.* **2011**, *11*, 3964−3978.
(37) *SAINT+*, v 6.2a; Bruker Analytical X-ray System, Inc., Madison, WI, 2001.
(38) *SADABS*; Bruker Analytical X-ray System, Inc., Madison, WI, 1999.
(39) Sheldrick, G. M. *SHELXTL*, v 6.10; Bruker Analytical X-ray Systems, Madison, WI, 2001.
(40) Macrae, C. F.; Edgington, P. R.; McCabe, P.; Pidcock, E.; Shields, G. P.; Taylor, R.; Towler, M.; van De Streek, J. *J. Appl. Crystallogr.* **2006**, *39*, 453−457.
(41) Dolomanov, O. V.; Bourhis, L. J.; Gildea, R. J.; Howard, J. A. K.; Puschmann, H. OLEX2: A complete structure solution, refinement and analysis program. *J. Appl. Crystallogr.* **2009**, *42*, 339−341.
(42) Timofeeva, T. V.; Kinnibrugh, T.; Borbulevych, O. Ya.; Averkiev, B. B.; Nesterov, V. N.; Sloan, A.; Antipin, M. Yu. *Cryst. Growth Des.* **2004**, *4*, 1265−1276.
(43) (a) Draguta, S.; Khrustalev, V. N.; Fonari, M. S.; Antipin, M. Y.; Timofeeva, T. V. *Acta Crystallogr.* **2012**, *E68*, o3353. (b) Draguta, S.; Leonova, E.; Fokina, M.; Denisyuk, I.; Timofeeva, T. V. *Acta Crystallogr.* **2013**, *E69*, o1280.
(44) Bernstein, J.; Davey, R. J.; Henck, J.-O. *Angew. Chem., Int. Ed.* **1999**, *38*, 3440−3461.
(45) Timofeeva, T. V.; Nesterov, V. N.; Dolgushin, F. M.; Zubavichus, Y. V.; Goldshtein, J. T.; Sammeth, D. M.; Clark, R. D.; Penn, B.; Antipin, M. Yu. *Cryst. Eng.* **2000**, *3*, 263−288.
(46) Yu, L. *Acc. Chem. Res.* **2010**, *43*, 1257−1266.
(47) Van Eijck, B. P.; Kroon, J. *Acta Crystallogr., Sect. B* **2000**, *56*, 535−542.
(48) Rodrigues, V. H.; Costa, M. M. R. R.; Belsley, M.; Gomes, E. M. *Acta Crystallogr. Sect. E* **2012**, *68*, o920.
(49) Etter, M. *Acc. Chem. Res.* **1990**, *23*, 120−126.
(50) Sreekanth, B. R.; Vishweshwar, P.; Vyas, K. *Chem. Commun.* **2007**, 2375−2377.
(51) Mukherjee, A.; Desiraju, G. R. *Chem. Commun.* **2011**, *47*, 4090−4092.
(52) Babu, N. J.; Cherukuvada, S.; Thakuria, R.; Nangia, A. *Cryst. Growth Des.* **2010**, *4*, 1979−1989.
(53) Kitajgorodskij, A. I. *Molecular Crystals and Molecules*; Academic Press: New York, 1973.
(54) (a) Burger, A.; Ramberger, R. *Mikrochim. Acta* **1979**, *2*, 259−271. (b) Burger, A.; Ramberger, R. *Mikrochim. Acta* **1979**, *2*, 273−316.
(55) Brock, C. P. *Acta Crystallogr., Sect. B* **2002**, *58*, 1025−1031.
(56) Bilton, C.; Howard, J. A.K.; Madhavi, N. N.L.; Nangia, A.; Desiraju, G. R.; Allen, F. H.; Wilson, C. C. *Chem. Commun.* **1999**, 1675−1676.
(57) Madura, I. D.; Czerwińska, K.; Jakubczyk, M.; Pawełko, A.; Adamczyk-Woźniak, A.; Sporzyński, A. *Cryst. Growth Des.* **2013**, *13*, 5344−5352.
(58) Nichol, G. L.; Clegg, W. *Cryst. Growth Des.* **2006**, *6*, 451−460.
(59) Chakraborty, S.; Rajput, L.; Desiraju, G. R. *Cryst. Growth Des.* **2014**, *14*, 2471−2577.
(60) Li, P.; Zhao, C.; Smith, M. D.; Shimizu, K. D. *J. Org. Chem.* **2013**, *78*, 5303−5313.
(61) Ringer, A. L.; Sherrill, C. D. *J. Am. Chem. Soc.* **2009**, *131*, 4574−4575.
(62) Babu, N. J.; Reddy, L. S.; Aitipamula, S.; Nangia, A. *Chem.—Asian J.* **2008**, *3*, 1122−1133.
(63) Zhang, S.-W.; Harasimowicz, M. T.; de Villiers, M. M.; Yu, L. *J. Am. Chem. Soc.* **2013**, *135*, 18981−18989.
(64) Yan, Y.; Hughes, C. E.; Kariuki, B. M.; Harris, K. D. M. *Cryst. Growth Des.* **2013**, *13*, 27−30.
(65) André, V.; Duarte, M. T.; Braga, D.; Grepioni, F. *Cryst. Growth Des.* **2012**, *12*, 3082−3090.
(66) Orola, L.; Veidis, M. V. *CrystEngComm* **2009**, *11*, 415−417.
(67) Lemmerer, A.; Adsmond, D. A.; Esterhuysen, C.; Bernstein, J. *Cryst. Growth Des.* **2013**, *13*, 3935−3952.